

Accessing the entire overdoped regime in pristine $\text{YBa}_2\text{Cu}_3\text{O}_{6+x}$ by application of pressure

P. L. Alireza,¹ G. H. Zhang,^{1,2} W. Guo,¹ J. Porras,³ T. Loew,³ Y.-T. Hsu,¹ G. G. Lonzarich,¹
M. Le Tacon,^{3,4} B. Keimer,³ and Suchitra E. Sebastian^{1,*}

¹*Cavendish Laboratory, Cambridge University, JJ Thomson Avenue, Cambridge CB3 0HE, United Kingdom*

²*Department of Physics, Massachusetts Institute of Technology, Cambridge, Massachusetts 02139, USA*

³*Max-Planck-Institut für Festkörperforschung, Heisenbergstrasse 1, D-70569 Stuttgart, Germany*

⁴*Karlsruher Institut für Technologie, Institut für Festkörperphysik, Hermann-v.-Helmholtz-Platz 1, D-76344 Eggenstein-Leopoldshafen, Germany*

(Received 31 October 2016; revised manuscript received 23 January 2017; published 27 March 2017)

We uncover the previously inaccessible overdoped regime to attain the complete superconducting dome in a pristine high temperature cuprate superconductor, by applying pressures up to 280 kbar to single crystals near stoichiometric $\text{YBa}_2\text{Cu}_3\text{O}_7$. The obtained superconducting phase boundary as a function of hole doping closely follows the form of the superconducting dome in $\text{La}_{2-x}\text{Sr}_x\text{CuO}_4$. Measurements are now enabled to trace the evolution of various entangled phases and the Fermi surface from the underdoped to overdoped regime in a single high purity cuprate superconducting family of materials.

DOI: [10.1103/PhysRevB.95.100505](https://doi.org/10.1103/PhysRevB.95.100505)

Copper oxide high temperature superconductors, while showing apparently conventional Fermi liquid behavior in the overdoped region of the phase diagram, exhibit a mysterious plethora of phases in the underdoped region of the phase diagram. In addition to d -wave superconductivity and Mott insulating antiferromagnetism, phases identified in the underdoped region include various forms of charge density wave, spin density wave, electronic nematic order, and a puzzling pseudogap region [1]. Recent studies have also suggested the potential deviation of superconducting behavior in the overdoped regime from the conventional Bardeen-Cooper-Schrieffer (BCS) theory [2–4]. Open questions remain regarding the relevance of the identified superconducting and density wave phases to the pseudogap region, and the evolution of each of these phases from the underdoped to the overdoped Fermi liquid-like region. An understanding of this evolution will shed light on the nature of the ill-understood pseudogap region, yet this has proved challenging thus far given the unavailability of pristine cuprate materials families that can be tuned across the entire superconducting phase diagram from underdoped to overdoped.

Among the high- T_c superconductors, $\text{YBa}_2\text{Cu}_3\text{O}_{6+x}$ (YBCO) (see inset of Fig. 1) is a material recognized for being clean and well ordered, which leads to its prevalence in quantum oscillation experiments and other measurements [5,6]. It has become one of the most extensively studied materials in the cuprate family, having well-identified critical points [7] and electronic orders [8–12]. While quantum oscillations and transport have been thoroughly studied in underdoped YBCO [13–15], similar measurements cannot be extended to the overdoped regime in the same material, despite having been successfully used to study the Fermi surface of a different cuprate, $\text{Tl}_2\text{Ba}_2\text{CuO}_{6+x}$ (Tl-2201) [16,17]. This is due to the fact that chemical doping in YBCO can only achieve a maximum hole concentration of 19.4% with oxygen tuning, and up to 22% with calcium substitution [18]. It is important to find a control parameter that can tune YBCO

into the overdoped region in a pristine way in order to track the evolution of the various forms of order and their relation to the pseudogap across the full range of doping, as well as to investigate the overdoped region itself. Hydrostatic pressure has been used as a tuning parameter [19,20] in past experiments to tune between adjoining electronic phases in materials, where the doping or bandwidth was found to change significantly with pressure [21]. For instance, pressure has both induced superconductivity and suppressed competing orders in magnetic materials such as UGe_2 [22–27], and revealed in CePd_2Si_2 and CeIn_3 critical points as a function of pressure (doping) that are relevant to superconductivity [28,29]. We report that by starting near $\text{YBa}_2\text{Cu}_3\text{O}_7$ and applying high pressures of up to 280 kbar, we have tuned the material into the heavily overdoped region up to a hole doping of $\approx 26\%$, where the superconducting transition temperature becomes almost fully suppressed. Thus, by using applied pressure as the control parameter in YBCO, we have achieved unprecedented access to the entire superconducting dome in a pristine high temperature superconducting material.

Applied pressure has been used as an effective control parameter for cuprates; resistivity measurements in $\text{Bi}_{1.98}\text{Sr}_{2.06}\text{Y}_{0.68}\text{CaCu}_2\text{O}_{8+x}$ have demonstrated pressure-induced superconductivity [30], while pressure-tuned Raman and x-ray diffraction data have indicated quantum critical points corresponding to electronic transitions [31]. For YBCO specifically, hydrostatic pressure has been applied up to 170 kbar on an initially underdoped sample with $x = 0.66$ and up to 110 kbar on an initially optimally doped sample with $x = 0.95$, showing pressure to affect the superconducting critical temperature in both cases. In the former, the effects of pressure, applied in the underdoped region, are complicated by oxygen ordering and thus difficult to analyze while the latter achieves a maximum effective n_h of around 0.2 which ventures into the slightly overdoped region [32,33]. Previous studies of YBCO under lower applied pressures have shown that increasing hydrostatic pressure decreases the distance between the BaO and CuO_2 planes, compressing the softer Cu(plane)-O bond and elongating the stiffer Cu(chain)-O bond (see inset of Fig. 1), thus increasing the number of holes per

*ses59@cam.ac.uk

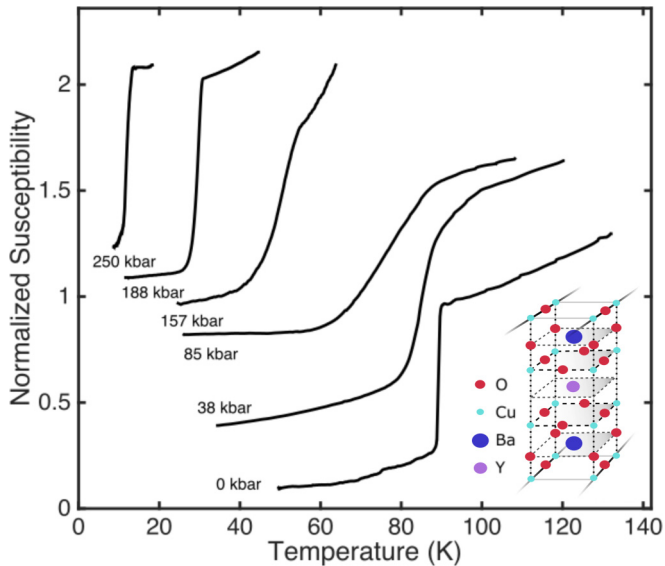


FIG. 1. Progression of ac susceptibility curves for single crystal $\text{YBa}_2\text{Cu}_3\text{O}_{6.98}$ with increasing applied pressure. Measurements were taken over multiple runs, by increasing pressure in the same setup or by remounting the sample at a higher pressure in a new setup. The inset shows the YBCO unit cell.

Cu atom in the CuO_2 plane (n_h) through hole transfer from the CuO chains [34,35]. Effects of pressure on T_c through induced structural phase transitions, oxygen ordering, and changes in the effective interaction strength [36–38] are in practice expected to be negligible above the slightly overdoped region [32,33,39]. This motivates our starting point for pressure tuning of stoichiometric $\text{YBa}_2\text{Cu}_3\text{O}_7$ in which the hole fraction is intrinsically just above optimal. This starting point enables us to most effectively access the highly overdoped regime using applied pressure, and ensures that the effect of pressure is principally to tune material properties via doping.

Single crystals of $\text{YBa}_2\text{Cu}_3\text{O}_{6+x}$ with $x = 0.98$ were grown out of solution and detwinned under uniaxial pressure [40]. The nominal oxygen content was determined by relating the superconducting temperature to the hole doping and oxygen concentration using the previously determined relationship for this material [18]. Polycrystalline $\text{YBa}_2\text{Cu}_3\text{O}_7$ was grown by conventional solid state reaction followed by sintering and cooling, according to methods described in previous literature [41]. To determine the effect of pressure on the superconducting transition temperature, we measured ac susceptibility in a diamond anvil cell (DAC) using a microcoil system [42]. Pressures of up to 300 kbar were generated using 0.6 mm culet diamonds with glycerol as the pressure medium. The sample space was a 200 μm hole drilled into a MP35 gasket, in which the signal coil, a 130 μm diameter, four turn microcoil made with 10 μm insulated copper wire, was placed. The drive coil, a 130 turn coil made with 30 μm insulated copper wire, was placed outside the pressure region. Pressure inside the sample space was determined by the ruby fluorescence method at room temperature and in some instances verified by the superconducting transition temperature of a lead sample at low temperatures. Additional measurements on dc magnetization were performed using a SQUID anvil cell

TABLE I. Superconducting temperatures obtained from ac susceptibility measurements on YBCO under several values of applied pressure, obtained from Fig. 1. The left side of the table shows results on single crystal YBCO and the right side of the table shows results on polycrystalline YBCO, which are found to be similar.

Single crystal YBCO		Polycrystalline YBCO	
Pressure (kbar)	T_c (K)	Pressure (kbar)	T_c (K)
0	89.1 ± 0.2	5	84.8 ± 0.3
38	85.1 ± 0.9	17	85.5 ± 0.3
85	76 ± 2	34	83.7 ± 0.6
90	70 ± 2	64	83.7 ± 0.9
113	68 ± 3	90	72 ± 2
157	49 ± 1	143	66 ± 5
188	29.3 ± 0.2	172	49 ± 6
204	28 ± 2	205	38 ± 2
250	12.0 ± 0.2	240	23.4 ± 0.6
280	7.34 ± 0.04	270	8.7 ± 0.2

specifically developed to be used in a Quantum Design MPMS system [43,44]. The cell, gasket, and pressure medium were set up similar to the one described above, using 0.6 mm diamond anvils, MP35 gasket, and glycerol as the pressure medium.

Ac susceptibility curves measured for both single crystal and polycrystalline YBCO at several values of applied pressure are shown in Fig. 1, where the susceptibilities have been normalized. We define the superconducting temperature as corresponding to the midpoint of the ac susceptibility curve. We find, as shown in Table I and Fig. 2, that up to applied pressures of around 90 kbar, the evolution in

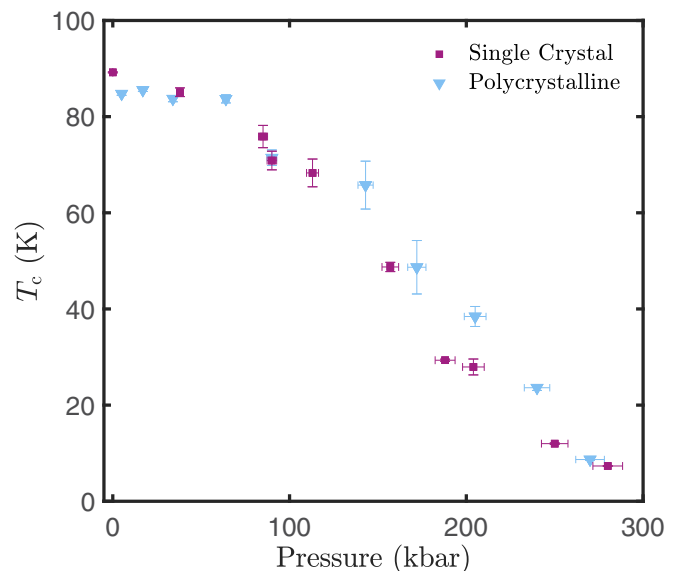


FIG. 2. Determination of T_c from ac susceptibility curves shows the decrease of transition temperature with increasing pressure for both single crystal and polycrystalline YBCO. Each point has a horizontal error of ± 2 kbar or $\pm 3\%$, the greater of which indicates uncertainty in the determination of pressure inside the sample space as described above. The vertical error bar corresponds to uncertainty in T_c , which is related to the width of the transition.

superconducting temperature is modest, falling by $\approx 20\%$, similar to that previously reported [33]. However, at higher values of applied pressures beyond those previously reported, the superconducting transition temperature begins to drop rapidly. For significantly high pressures up to 280 kbar, we find that superconductivity is almost destroyed, with the superconducting temperature falling to below 10 K. It is clear that, in the case of YBCO, the large energy scales that characterize this material necessitate extremely high applied pressures far beyond those achieved in previous studies to access the overdoped region of the phase diagram. Superconducting transition temperatures as a function of applied pressure are found to be similar for single crystal and polycrystalline YBCO, demonstrating the suppression of superconductivity to be primarily a volume effect rather than a uniaxial effect. The width of the superconducting transition under pressure reflects both the gasket condition during the run and the level of pressure homogeneity within the sample. The remarkable sharpness of the superconducting transitions we observe at the highest applied pressures in the vicinity of 250 kbar (Fig. 1) demonstrates the high homogeneity of pressure conditions we have been able to achieve even at these very high pressures.

In order to map the YBCO phase diagram with T_c as a function of n_h for our applied pressure measurements, we translate applied pressure into hole doping. Pressure effects separate into that of charge transfer and those unrelated to changes in doping [39]. The latter effects peak in the underdoped region in a manner that has been attributed to oxygen ordering and other factors [33], and drastically diminish as n_h is increased from underdoping to overdoping. Charge transfer effects therefore dominate in the overdoped regime that we study [32]. Thus, in our analysis of overdoped YBCO, we focus on the effect of pressure through doping. Early pressure studies done in the overdoped regime, which similarly assume negligibility of doping-independent contributions, show the effect of pressure on the change in n_h to closely correspond to a linear dependence on the relative decrease in cell volume [46–48]. We follow similar analysis, denoting the relative decrease in the unit cell volume as $\xi(P) \equiv (1 - V(P)/V_0)$, where V is the cell volume, P is the applied pressure, and V_0 is the cell volume at zero pressure. Using the first-order Murnaghan equation [49], we assume

$$\frac{dn_h(P)}{d\xi(P)} = n'_h(P)B_0 \left(1 + \frac{B'_0}{B_0}P\right)^{1+1/B'_0}, \quad (1)$$

$$\xi(P) = 1 - \left(1 + \frac{B'_0}{B_0}P\right)^{-1/B'_0}, \quad (2)$$

where $n'_h(P) = dn_h(P)/dP$ and $n_{h,0}$, B_0 , and B'_0 are, respectively, the initial hole doping, bulk modulus $-V(dP/dV)$, and pressure derivative of the bulk modulus at zero pressure. The initial doping $n_h(0) = 0.19$ holes/Cu was found by locating T_c on the $\text{La}_{2-x}\text{Sr}_x\text{CuO}_4$ (LSCO) superconducting dome, $1 - T_c/T_{c,\max} = 82.6(n_h - 0.16)^2$ with $T_{c,\max} = 94.3$ K for YBCO single crystals [18]. Values considered for B_0 and B'_0 were taken from previous pressure studies using x-ray analysis, on samples with oxygen content close to that of our single crystals $x = 0.98$; as such, we assume a range of $B_0 = 1306 \pm$

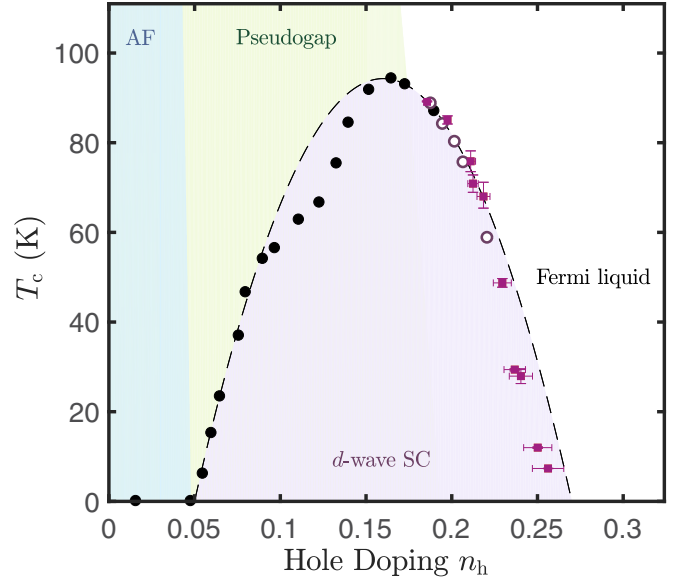


FIG. 3. T_c -doping phase diagram for single crystal YBCO, with translated pressure-tuned data from Fig. 2 (squares), previous pressure-tuned data (hollow circles) [45], and previous zero-pressure data (filled circles) [18]. Translation from pressure to doping n_h was done using relations (1) and (2) while considering constraints in accordance with previous data on $\text{Y}_{1-x}\text{Ca}_x\text{Ba}_2\text{Cu}_3\text{O}_{6.96}$ [45], for which n_h was estimated using a combination of copper and oxygen bond valence sums (BVS). The effects of the different constraints are reflected in the horizontal error bars. The dashed curve indicates the LSCO superconducting dome [2,45], $1 - T_c/T_{c,\max} = 82.6(n_h - 0.16)^2$, with $T_{c,\max}$ set to 94.3 K for YBCO single crystals [18].

11 kbar and $B'_0 = 4.8 \pm 0.2$ to $B_0 = 1500$ kbar and $B'_0 = 4$, obtained for $x = 0.95$ [50] and $x = 1$ [51], respectively. Starting with an assumption of parabolic dependence of the superconducting temperature as a function of hole doping up to $n_h = 0.22$ similar to previous work [45], we apply relations (1) and (2) (see Supplemental Material [52] for further details of the calculation) to yield the dependence of the superconducting temperature as a function of n_h at higher dopings. The full superconducting phase diagram thus obtained as a function of hole doping is shown in Fig. 3. We are therefore able to map the full superconducting dome in a pristine way in a high temperature cuprate superconductor by applied pressure tuning starting near stoichiometric $\text{YBa}_2\text{Cu}_3\text{O}_7$. Importantly, we find that the superconducting temperature dependence on hole doping is in good agreement with the form of the superconducting dome mapped in the LSCO cuprates [53–55].

Crucially, our applied pressure measurements provide unprecedented access beyond the optimally doped region in YBCO, allowing for measurements of quantum oscillations, electrical and thermal transport, magnetization, penetration depth, and other properties in the overdoped regime of this family of high- T_c materials. In particular, we expect to trace the evolution of the Fermi surface pockets from small to large across the entire phase diagram, and to resolve each of the entangled density wave and d -wave superconducting phases from the underdoped to the overdoped region, as well as their relation to each other and the pseudogap region, in

this family of high- T_c cuprates. Another important question to be addressed pertains to the robustness of superconductivity with increasing temperature and applied magnetic field in the underdoped region compared to that in the overdoped region. Controversy surrounds whether superconductivity persists to high magnetic fields in the underdoped regime, as would be characteristic of strongly coupled superconductivity in proximity to the Mott transition [56], or whether superconductivity in the underdoped regime is suppressed by modest critical magnetic fields as would be characteristic of conventional BCS superconductivity [57]. Recent studies have also challenged the Fermi liquid character of the overdoped regime [2,4]. We

can shed light on this issue by a comparative study of the nature of superconductivity in the underdoped regime, and the overdoped regime of YBCO we now access.

P.L.A., G.H.Z., W.G., Y.T.H., and S.E.S. acknowledge support from the Royal Society, the Winton Programme for the Physics of Sustainability, and the European Research Council under the European Union's Seventh Framework Programme (Grant No. FP/2007-2013)/ERC Grant Agreement No. 337425 and EPSRC Grant No. EP/M000524/1. G.H.Z. acknowledges support from the Cambridge-MIT Exchange Program. G.G.L. acknowledges support from EPSRC Grant No. EP/K012894/1.

-
- [1] B. Keimer, S. A. Kivelson, M. R. Norman, S. Uchida, and J. Zaanen, *Nature (London)* **518**, 179 (2015).
- [2] I. Božović, X. He, J. Wu, and A. T. Bollinger, *Nature (London)* **536**, 309 (2016).
- [3] D. C. Peets, D. G. Hawthorn, K. M. Shen, Y.-J. Kim, D. S. Ellis, H. Zhang, S. Komiya, Y. Ando, G. A. Sawatzky, R. Liang, D. A. Bonn, and W. N. Hardy, *Phys. Rev. Lett.* **103**, 087402 (2009).
- [4] A. Gauzzi, Y. Klein, M. Nisula, M. Karppinen, P. K. Biswas, H. Saadaoui, E. Morenzoni, P. Manuel, D. Khalyavin, M. Marezio, and T. H. Geballe, *Phys. Rev. B* **94**, 180509 (2016).
- [5] S. E. Sebastian and C. Proust, *Annu. Rev. Condens. Matter Phys.* **6**, 411 (2015).
- [6] S. E. Sebastian, N. Harrison, and G. G. Lonzarich, *Rep. Prog. Phys.* **75**, 102501 (2012).
- [7] J. L. Tallon and J. W. Loram, *Phys. C: Supercond.* **349**, 53 (2001).
- [8] D. Fournier, G. Levy, Y. Pennec, J. L. McChesney, A. Bostwick, E. Rotenberg, R. Liang, W. N. Hardy, D. A. Bonn, I. S. Elfimov, and A. Damascelli, *Nat. Phys.* **6**, 905 (2010).
- [9] T. Wu, H. Mayaffre, S. Kramer, M. Horvatic, C. Berthier, W. N. Hardy, R. Liang, D. A. Bonn, and M.-H. Julien, *Nature (London)* **477**, 191 (2011).
- [10] M. Hücker, N. B. Christensen, A. T. Holmes, E. Blackburn, E. M. Forgan, R. Liang, D. A. Bonn, W. N. Hardy, O. Gutowski, M. v. Zimmermann, S. M. Hayden, and J. Chang, *Phys. Rev. B* **90**, 054514 (2014).
- [11] S. Blanco-Canosa, A. Frano, E. Schierle, J. Porras, T. Loew, M. Minola, M. Bluschke, E. Weschke, B. Keimer, and M. Le Tacon, *Phys. Rev. B* **90**, 054513 (2014).
- [12] T. Wu, H. Mayaffre, S. Krämer, M. Horvatic, C. Berthier, P. L. Kuhns, A. P. Reyes, R. Liang, W. N. Hardy, D. A. Bonn, and M.-H. Julien, *Nat. Commun.* **4**, 2113 (2013).
- [13] S. E. Sebastian, N. Harrison, F. F. Balakirev, M. M. Altarawneh, P. A. Goddard, R. Liang, D. A. Bonn, W. N. Hardy, and G. G. Lonzarich, *Nature (London)* **511**, 61 (2014).
- [14] S. Badoux, W. Tabis, F. Laliberté, G. Grissonnanche, B. Vignolle, D. Vignolles, J. Béard, D. A. Bonn, W. N. Hardy, R. Liang, N. Doiron-Leyraud, L. Taillefer, and C. Proust, *Nature (London)* **531**, 210 (2016).
- [15] Y. Ando, Y. Kurita, S. Komiya, S. Ono, and K. Segawa, *Phys. Rev. Lett.* **92**, 197001 (2004).
- [16] B. Vignolle, A. Carrington, R. A. Cooper, M. M. J. French, A. P. Mackenzie, C. Jaudet, D. Vignolles, C. Proust, and N. E. Hussey, *Nature (London)* **455**, 952 (2008).
- [17] A. F. Bangura, P. M. C. Rourke, T. M. Benseman, M. Matusiak, J. R. Cooper, N. E. Hussey, and A. Carrington, *Phys. Rev. B* **82**, 140501 (2010).
- [18] R. Liang, D. A. Bonn, and W. N. Hardy, *Phys. Rev. B* **73**, 180505 (2006).
- [19] G. G. Lonzarich, in *Electron*, edited by M. Springford (Cambridge University Press, Cambridge, UK, 1997), Chap. 6.
- [20] H. Fukuyama, *Rev. High Press. Sci. Technol.* **7**, 465 (1998).
- [21] F. M. Grosche, S. R. Julian, N. D. Mathur, and G. G. Lonzarich, *Physica B* **223–224**, 50 (1996).
- [22] N. D. Mathur, F. M. Grosche, S. R. Julian, I. R. Walker, D. M. Freye, R. K. W. Haselwimmer, and G. G. Lonzarich, *Nature (London)* **394**, 39 (1998).
- [23] S. S. Saxena, P. Agarwal, K. Ahilan, F. M. Grosche, R. K. W. Haselwimmer, M. J. Steiner, E. Pugh, I. R. Walker, S. R. Julian, P. Monthoux, G. G. Lonzarich, A. Huxley, I. Sheikin, D. Braithwaite, and J. Flouquet, *Nature (London)* **406**, 587 (2000).
- [24] G. Oomi, T. Kagayama, and Y. Onuki, *J. Alloys Compd.* **271–273**, 482 (1998).
- [25] K. Nishimura, G. Oomi, S. W. Yun, and Y. Onuki, *J. Alloys Compd.* **213–214**, 383 (1994).
- [26] A. Huxley, I. Sheikin, and D. Braithwaite, *Physica B* **284–288**, 1277 (2000).
- [27] M. Leroux, I. Errea, M. Le Tacon, S.-M. Souliou, G. Garbarino, L. Cario, A. Bosak, F. Mauri, M. Calandra, and P. Rodière, *Phys. Rev. B* **92**, 140303 (2015).
- [28] J. D. Thompson, R. D. Parks, and H. Borges, *J. Magn. Magn. Mater.* **54–57**, 377 (1986).
- [29] J. Flouquet, *J. Magn. Magn. Mater.* **90–91**, 377 (1990).
- [30] T. Cuk, D. A. Zocco, H. Eisaki, V. Struzhkin, F. M. Grosche, M. B. Maple, and Z. X. Shen, *Phys. Rev. B* **81**, 184509 (2010).
- [31] T. Cuk, V. V. Struzhkin, T. P. Devereaux, A. F. Goncharov, C. A. Kendziora, H. Eisaki, H.-K. Mao, and Z.-X. Shen, *Phys. Rev. Lett.* **100**, 217003 (2008).
- [32] O. Cyr-Choinière, D. LeBoeuf, S. Badoux, S. Dufour-Beauséjour, D. A. Bonn, W. N. Hardy, R. Liang, N. Doiron-Leyraud, and L. Taillefer, [arXiv:1503.02033](https://arxiv.org/abs/1503.02033).
- [33] S. Sadewasser, J. S. Schilling, A. P. Paulikas, and B. W. Veal, *Phys. Rev. B* **61**, 741 (2000).
- [34] J. Jorgensen, S. Pei, P. Lightfoot, D. Hinks, B. Veal, B. Dabrowski, A. Paulikas, R. Kleb, and I. Brown, *Phys. C: Supercond.* **171**, 93 (1990).

- [35] Y. Yamada, J. D. Jorgensen, S. Pei, P. Lightfoot, Y. Kodama, T. Matsumoto, and F. Izumi, *Phys. C: Supercond.* **173**, 185 (1991).
- [36] S. W. Tozer, J. L. Koston, and E. M. McCarron III, *Phys. Rev. B* **47**, 8089 (1993).
- [37] J. Schilling, in *Handbook of High Temperature Superconductivity: Theory and Experiment*, edited by J. Schrieffer and J. Brooks (Springer-Verlag, Hamburg, 2007), Chap. 11.
- [38] S. M. Souliou, A. Subedi, Y. T. Song, C. T. Lin, K. Syassen, B. Keimer, and M. Le Tacon, *Phys. Rev. B* **90**, 140501 (2014).
- [39] B. Lorenz and C. Chu, in *Frontiers in Superconducting Materials*, edited by A. Narlikar (Springer-Verlag, Berlin, 2005), pp. 459–497.
- [40] C. T. Lin, W. Zhou, W. Y. Liang, E. Schönherr, and H. Bender, *Phys. C: Supercond.* **195**, 291 (1992).
- [41] S. Zagoulaev, P. Monod, and J. Jégoudez, *Phys. Rev. B* **52**, 10474 (1995).
- [42] P. L. Alireza and S. R. Julian, *Rev. Sci. Instrum.* **74**, 4728 (2003).
- [43] P. L. Alireza and G. G. Lonzarich, *Rev. Sci. Instrum.* **80**, 023906 (2009).
- [44] P. L. Alireza, S. Barakat, A.-M. Cumberlidge, G. Lonzarich, F. Nakamura, and Y. Maeno, *J. Phys. Soc. Jpn.* **76**, 216 (2007).
- [45] J. L. Tallon, C. Bernhard, H. Shaked, R. L. Hitterman, and J. D. Jorgensen, *Phys. Rev. B* **51**, 12911 (1995).
- [46] X.-J. Chen, V. V. Struzhkin, R. J. Hemley, H.-k. Mao, and C. Kendziora, *Phys. Rev. B* **70**, 214502 (2004).
- [47] X. J. Chen, H. Q. Lin, and C. D. Gong, *Phys. Rev. Lett.* **85**, 2180 (2000).
- [48] W. H. Fietz, F. W. Hornung, K. Grube, S. I. Schlachter, T. Wolf, B. Obst, and P. Schweiss, *J. Low Temp. Phys.* **117**, 915 (1999).
- [49] J. S. Olsen, S. Steenstrup, L. Gerward, and B. Sundqvist, *Phys. Scr.* **44**, 211 (1991).
- [50] I. V. Medvedeva, Y. S. Bersenev, B. A. Gizhevsky, N. M. Chebotaev, S. V. Naumov, and G. B. Demishev, *Z. Phys. B: Condens. Matter* **81**, 311 (1990).
- [51] H. Ludwig, W. Fietz, and H. Wühl, *Phys. C: Supercond.* **197**, 113 (1992).
- [52] See Supplemental Material at <http://link.aps.org/supplemental/10.1103/PhysRevB.95.100505> for details on the translation of applied pressure to hole doping.
- [53] J. B. Torrance, A. Bezing, A. I. Nazzal, T. C. Huang, S. S. P. Parkin, D. T. Keane, S. J. LaPlaca, P. M. Horn, and G. A. Held, *Phys. Rev. B* **40**, 8872 (1989).
- [54] H. Takagi, T. Ido, S. Ishibashi, M. Uota, S. Uchida, and Y. Tokura, *Phys. Rev. B* **40**, 2254 (1989).
- [55] M. Presland, J. Tallon, R. Buckley, R. Liu, and N. Flower, *Phys. C: Supercond.* **176**, 95 (1991).
- [56] L. Li, Y. Wang, S. Komiyama, S. Ono, Y. Ando, G. D. Gu, and N. P. Ong, *Phys. Rev. B* **81**, 054510 (2010).
- [57] G. Grissonnanche, O. Cyr-Choinière, F. Laliberté, S. Renéde Cotret, A. Juneau-Fecteau, S. Dufour-Beauséjour, M. È. Delage, D. LeBoeuf, J. Chang, B. J. Ramshaw, D. A. Bonn, W. N. Hardy, R. Liang, S. Adachi, N. E. Hussey, B. Vignolle, C. Proust, M. Sutherland, S. Krämer, J. H. Park, D. Graf, N. Doiron-Leyraud, and L. Taillefer, *Nat. Commun.* **5**, 3280 (2014).